

From Human Motion Analysis to Whole-Body Control of a Dual-Arm Robot for Pick-and-Place Tasks

Sung-Kyun Kim, Dong-hyun Lee, Seokmin Hong, Yonghwan Oh, Sang-Rok Oh

Abstract—Human’s action strategy is a good source of robot controller design. For there is no decisive criterion on balance control during manipulation tasks, human motion data are obtained and analyzed in this paper. Based on the observation of the center of mass (CoM) being proportional to target object distance but limited inside the supporting polygon, the bound-proportional CoM planner is proposed. Along with the CoM planner, whole-body balance and grasping controller for a dual-arm robot is suggested in a simple and computationally efficient structure. Dynamic simulation is conducted for validation, and showed competent results.

I. INTRODUCTION

Recently, many dual-arm robots are developed for service robot purposes, and a pick-and-place task would be one of most frequent tasks that are imposed to dual-arm robots. Not likely to industrial robots, service-purposed dual-arm robots are on mobile platforms or in a humanoid type. As they are not fixed on the ground, balance control is highly important while performing any tasks.

Whole-body balance control is intrinsically necessary, but difficult as well, since dual-arm robots usually have high degrees-of-freedom (DOFs). Moreover, there are no deterministic criteria on which is the best way to control the balance while executing the given tasks; to control the overall center-of-mass (CoM) to be at the center of supporting polygon or on the border of it.

Mobile manipulation area is deeply related to this topic of whole-body control during a manipulation task, but many of mobile manipulators have non-articulated body except the manipulator part, thus yielding the lack of self-balance ability. Most of works on mobile manipulation are still on connecting a manipulation task and path planning [1], [2], [3].

In humanoid robot research, whole-body control issue is more frequently addressed. However, there is a deficiency in the attempt to relate pick-and-place task and whole-body control. There are abundant researches on motion planning for pick-and-place tasks, but balance control is not considered, and many of their algorithms utilize an inverse kinematics method which is computationally expensive, especially for redundant systems [4], [5], [6]. Also, whole-body control of a humanoid robot is another huge area, but

Sung-Kyun Kim, Dong-hyun Lee, Yonghwan Oh and Sang-Rok Oh are with the Interaction and Robotics Research Center in Korea Institute of Science and Technology (KIST), Korea {kimsk, 022759, oyh, sroh}@kist.re.kr

Seokmin Hong is with Korea University of Science and Technology (UST) and the Interaction and Robotics Research Center in Korea Institute of Science and Technology (KIST), Korea {doberman77}@kist.re.kr

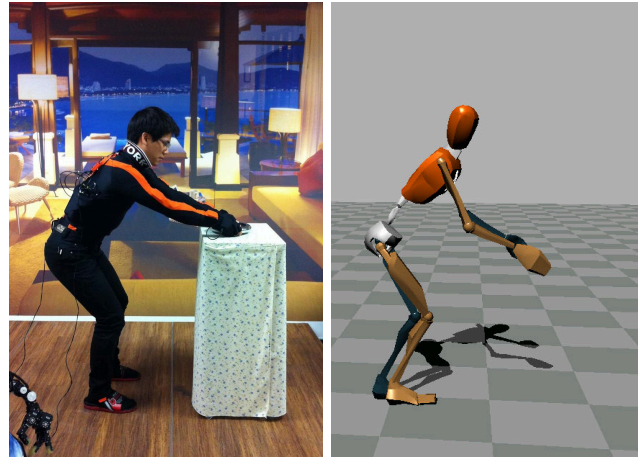


Fig. 1. Inertial measurement unit (IMU)-based motion capture system (left) and the graphical model of captured data (right).

its balance control purpose remains rather simple for various tasks. There are great works on humanoid robot balancing for picking an object from the ground or lifting a large object, but the control goal is just to maintain the overall CoM at the center of the supporting polygon [7], [8], [9], [10].

Then, it is worthy to look into humans how they do pick-and-place tasks while keeping the balance. Many physiologists have studied on a variety of human motions including reaching [11], [12], [13] and balancing motions [14], [15]. Their study revealed the coordination of arm and trunk motions and the balance strategy during swaying motions, but not in together, which means that there is a limitation to use these specific data for pick-and-place motion analysis with the consideration on balance control.

In this paper, human motions for pick-and-place tasks are obtained and analyzed in order to deduce the balance strategy during reaching motions, and the strategy is applied to the whole-body controller of a dual-arm robot. Based on the previous works of the authors [16], [17], [18], task-space feedback control scheme is used in the controller for both of the end-effector and the CoM positions, which is in a simple structure and provides compliant and human-like motions.

Acquisition and analysis of pick-and-place human motions are described in section II, and the balance strategy and whole-body controller are proposed in section III. To validate the proposed method, dynamic simulation of a dual-arm robot is conducted for pick-and-place tasks in section IV, and section V concludes this paper.

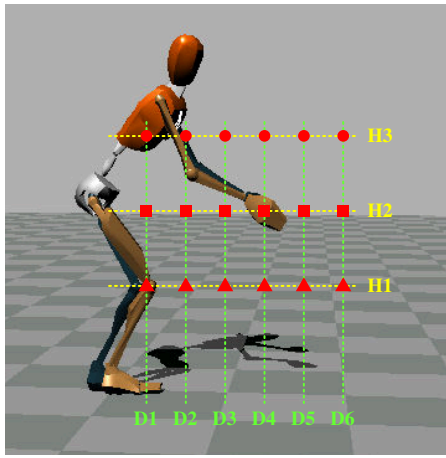


Fig. 2. Pick-and-place task assignment: $D_j \in \{0.15, 0.3, 0.45, 0.6, 0.75, 0.9\}$ [m] and $H_k \in \{0.4, 0.7, 1.0\}$ [m] for $M_i \in \{1, 3, 5\}$ [kg].

II. HUMAN MOTION ANALYSIS

A. Motion Capture System and Experiment Setup

The motion capture environment is comprised of a IMU-based motion capture system, workbenches in different heights and target objects in different weights (Fig. 1). A commercial motion capture system is used here; *MVN System* from *Xsens Technologies B.V.* Full-body motion data were obtained at 120 Hz, and adjusted according to a human anatomic model.

As depicted in Fig. 2, target objects in three kinds of weights are located at six kinds of distance and three kinds of heights. Three male subjects aged 25 to 29 years of 65 kg weight and 172 cm height on average participated in this study. The subjects were instructed to 'pick the target object', 'lift it in front of the chest', and 'place it at the original position' while they stand on a flat floor. Herein, only planar motions on the sagittal plane are considered.

The dynamics for the obtained motion data is computed based on inertial property of a mid-size anatomic model described in [19] which has five links in torso and three links in each limb. Zero moment point (ZMP) is obtained using the method in [20].

B. Human Motion Analysis for Pick-and-Place Tasks

In this section, the results of human motion analysis are provided. One sample of obtained pick-and-place motions are depicted in Fig. 3. A pick-and-place motion consists of four motion phases: 1) reaching to the object, 2) pick and lift it, 3) lower and place it, 4) return to the normal stance. Our interest is on the phase transition instants from 1) to 2) and from 3) to 4) when arms are stretched to the farthest reach such that the balance is at risk. These phase transition instants are detected from segmentation process which searches an instant at which the hand speed is at a local minimum.

The total CoM of the human body and an object is computed for the instant of each phase transition. ZMP which is an important parameter for balance control is also

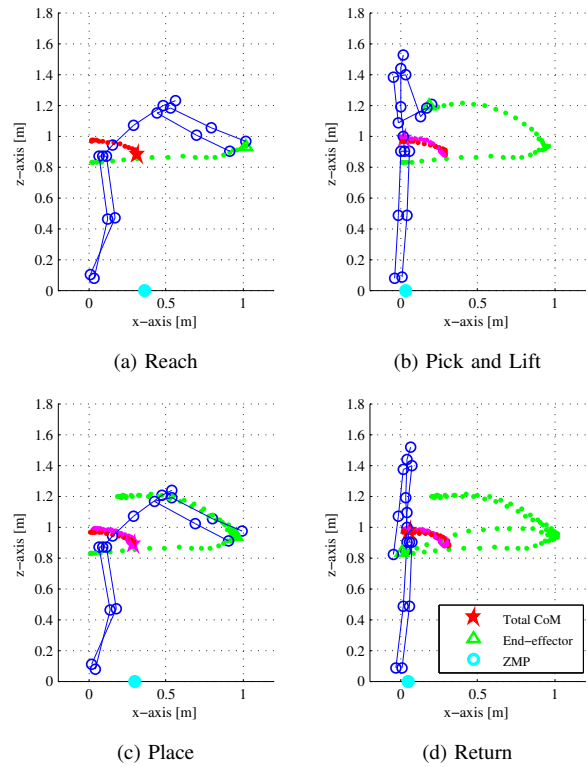


Fig. 3. Human motion trajectory for a pick-and-place task ($[M_i, D_j, H_k] = [3, 0.9, 1.0]$). During (b) and (c) phases, the CoM computation includes the object mass, and marked in magenta (light red).

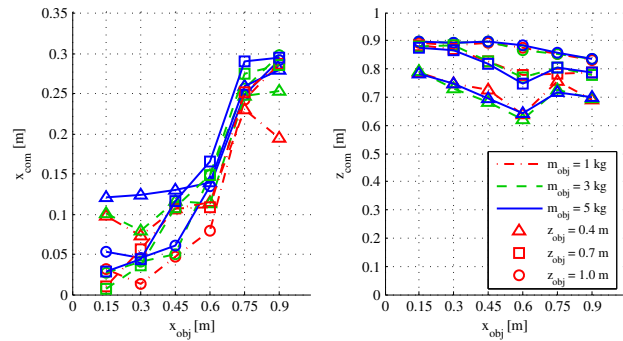


Fig. 4. Correlation between target object distance, x_{obj} , and total CoM position at the instants of reaching and placing, x_{com} and z_{com} , for all assigned tasks.

computed and depicted in the plot for the instant of each phase transition.

In Fig. 4 and Fig. 5, the total CoM positions at phase transitions are presented for the diverse assigned tasks. Fig. 5 describes the total CoM position more precisely in order to investigate individual correlations with several control parameters. The results reveals that x-position of the total CoM, x_{com} , has strong and approximately linear relation with x-position of the target object, x_{obj} and slight relation with object mass, m_{obj} , and with object z-position, z_{obj} . Z-position of the total CoM, z_{com} , is strongly related to z_{obj} , but not

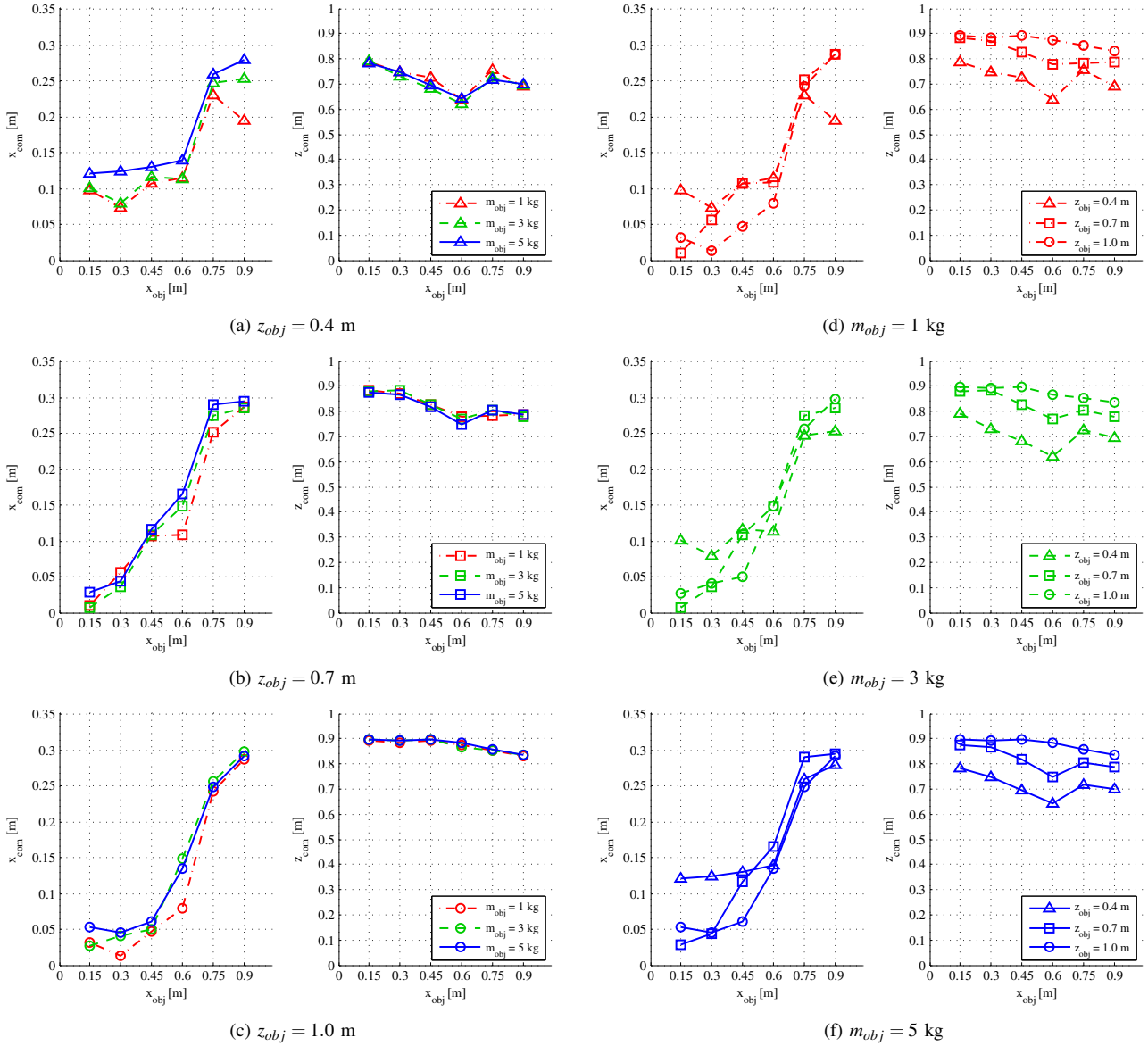


Fig. 5. Correlation between target object distance, x_{obj} , and total CoM position at the instants of reaching and placing, x_{com} and z_{com} , for different object masses, m_{obj} , and object heights, z_{obj} .

significantly related to x_{obj} nor m_{obj} .

Fig. 4 gives the overall impression of the correlation between x_{com} and x_{obj} , which shows that x_{com} has a proportional relation with x_{obj} although there is certain variation near to the origin of x -position possibly due to the DOF redundancy. Another important thing which should be noted is that x_{com} is bound even though x_{obj} increases. This seems to be a natural phenomenon to trap CoM inside the supporting polygon in order to maintain the balance.

III. WHOLE-BODY CONTROL WITH CoM PLANNER

A. Bound-Proportional CoM Planner

Based on the observation in section II-B, a bound-proportional CoM planner (BP-CoM planner) is proposed in this section. It is still reasonable for a robot to adopt a

proportional relation between a desired CoM position and a desired end-effector position, since CoM is basically to move toward the direction the end-effector moves. Moreover, the robot CoM is required to be bound inside the supporting polygon so that it may not fall down.

Such a BP-CoM planner can be formulated by combining a proportional linear function and a reciprocal of a polynomial function that has an asymptote at $x_{com} = b$;

$$x_{obj} = k_1 x_{com} + k_2 \frac{1}{x_{com}^n - b} \quad (1)$$

where k_1 is a proportional ratio of x_{obj} to x_{com} , k_2 is a parameter of contribution of the reciprocal polynomial function, and b implies the boundary of CoM. k_1 should be determined in regard of the ratio of the arm mass to the total mass and the preferred arm configuration in reaching

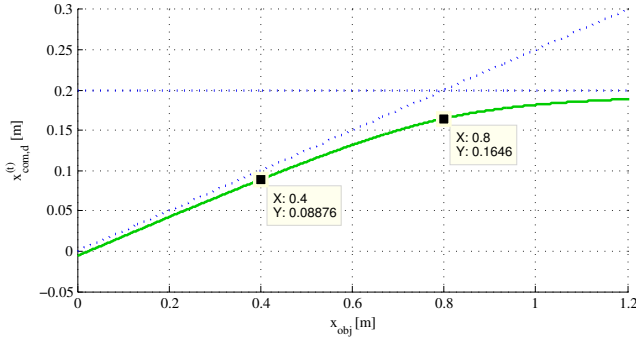


Fig. 6. Designed BP-CoM planner for a dual-arm robot with a base radius of 0.2 m.

motion. b can be selected by subtracting a desirable safety margin from the physical base of support (BoS) of the robot.

If we take n simply as $n = 1$, the desired total CoM of a robot and an object system, which is denoted with superscript (t), is determined for given target object position.

$$x_{com,d}^{(t)} = \frac{(x_{obj} + k_1 b) - \sqrt{(x_{obj} - k_1 b)^2 + 4k_1 k_2}}{2k_1}. \quad (2)$$

Then, the desired CoM of the robot, which is denoted with superscript (r), can be obtained from the following equations, considering the object grasping state:

$$x_{com,d}^{(r)} = \begin{cases} x_{com,d}^{(t)} & \text{(released)} \\ \frac{(m_{rob} + m_{obj})x_{com,d}^{(t)} - m_{obj}x_{obj}}{m_{rob}} & \text{(grasped)} \end{cases} \quad (3)$$

where m_{rob} and m_{obj} denote masses of the robot and the object, respectively.

B. Controller for a Dual-arm Robot

Whole-body balance and manipulation controller for a dual-arm robot is based on the task-space feedback scheme and end-effector impedance control which is suggested in [21], [22], [23]. This approach does not require computation of inverse of Jacobian matrix or system dynamics.

For joint position vector, $q = [q_0^T \ q_1^T \ q_2^T]^T$ where q_0 , q_1 and q_2 imply joint position vectors of torso, left arm and right arm, respectively, let us denote $q_{01} = [q_0^T \ q_1^T]^T$, $q_{02} = [q_0^T \ q_2^T]^T$. Then the end-effector Jacobian matrices, J_{01} and J_{02} , and the CoM Jacobian matrix, J_{com} are obtained as follows:

$$J_{01} = \frac{\partial x_{end,1}}{\partial q_{01}} = \begin{bmatrix} J_{01,0} \\ J_{01,1} \end{bmatrix} \rightarrow J_1 = \begin{bmatrix} J_{01,0} \\ J_{01,1} \\ 0_{n_2 \times 3} \end{bmatrix}, \quad (4)$$

$$J_{02} = \frac{\partial x_{end,2}}{\partial q_{02}} = \begin{bmatrix} J_{02,0} \\ J_{02,2} \end{bmatrix} \rightarrow J_2 = \begin{bmatrix} J_{02,0} \\ 0_{n_1 \times 3} \\ J_{02,2} \end{bmatrix}, \quad (5)$$

$$J_{com} = \frac{\partial x_{com}^{(r)}}{\partial q} \quad (6)$$

where n_0 , n_1 and n_2 mean the DOF of each part, and J_1 and J_2 represent augmented Jacobians in $(n_0 + n_1 + n_2)$ -by-3 matrix.

The joint command torque vectors, u_{01} and u_{02} , are computed according to the following controller:

$$\begin{aligned} u_{0i} = & -C\dot{q} + J_i^T (-c_{end}\dot{x}_{end,i} + k_{end}\Delta x_{end,i}) \\ & + \frac{1}{2}J_{com}^T (-c_{com}\dot{x}_{com}^{(r)} + k_{com}\Delta x_{com}^{(r)}) \\ & + (-1)^i \delta[i_{gsp}]J_i^T k_{gsp} \frac{x_{end,1} - x_{end,2}}{\|x_{end,1} - x_{end,2}\|} \end{aligned} \quad (7)$$

for $i = 1, 2$, where C is a diagonal matrix of joint damping coefficients, c_{end} and c_{com} are task-space damping, and k_{end} and k_{com} are task-space spring stiffness for the end-effector and the CoM, respectively. k_{gsp} implies a grasping force coefficient, and $\Delta x_{end,i} = x_{end,i,d} - x_{end,i}$ and $\Delta x_{com}^{(r)} = x_{com,d}^{(r)} - x_{com}^{(r)}$ denote position errors of the i -th end-effector and the robot CoM, respectively. $\delta[i_{gsp}]$ is a Kronecker delta function defined as follows:

$$\delta[i_{gsp}] = \begin{cases} 0 & (i_{gsp} = 1; \text{released}) \\ 1 & (i_{gsp} = 0; \text{grasped}) \end{cases}. \quad (8)$$

In the right hand side of (7), the first term is joint-space damping for enhancing the system stability, the second and the third term are task-space feedback control input for end-effector and CoM positions, respectively, and the last term is grasping control input for the i -th limb.

Finally, the overall command torque vector, u , is obtained as follows:

$$u = \text{diag}[I_{n_0}, I_{n_1}, I_{n_2}](u_{01} + u_{02}). \quad (9)$$

C. Robustness of the Proposed Method

Robustness when picking a very heavy object or reaching to a very far distance is addressed here. There are two stages in performing the assigned pick-and-place task: CoM planning stage and set-point regulation stage.

1) *CoM Planning Stage:* The desired CoM for a given task is obtained from the BP-CoM Planner as (3). In order to keep the the whole-body balance during the task, this stage has to yield the desired CoM of the robot that is within the CoM workspace, $x_{com,d}^{(r)} \in X_{com}^{(r)} = \{x_{com}^{(r)}(q) | \forall q \text{ in workspace}\}$.

When the robot does not holding the object (released state), the desired robot CoM cannot be out of the CoM workspace, since it is the same as the desired total CoM which never exceed $X_{com}^{(r)}$ according to (2).

When the robot tries to hold the object (grasped state), it should be judged whether the robot can accomplish grasping or not, since the desired robot CoM may be out of the CoM workspace if m_{obj} or x_{obj} are too large. When the result is as $x_{com,d}^{(r)} \notin X_{com}^{(r)}$, it means that the given pick-and-place task cannot be achieved by the robot while maintaining its whole-body balance.

2) *Set-point Regulation Stage*: The overall system dynamics including the object can be presented as follows.

$$H(q)\ddot{q} + \left\{ \frac{1}{2}\dot{H}(q) + S(q, \dot{q}) \right\} \dot{q} + \sum_{i=1,2} J_i^T f_i = u, \quad (10)$$

$$m_{obj}\ddot{x}_{obj} - \sum_{i=1,2} f_i = 0, \quad (11)$$

$$I_{obj}\dot{\omega}_{obj} + \omega_{obj} \times I_{obj}\omega_{obj} - \sum_{i=1,2} x_{obj,i} \times f_i = 0 \quad (12)$$

for $i = 1, 2$, where $H(q)$ is the robot inertia matrix, and $S(q, \dot{q})$ is a skew-symmetric matrix for centrifugal and Coriolis forces. Note that $x_{obj,i}$ is a position vector from x_{obj} to the contact position between the object and the i -th end-effector, and f_i is a force applied by the end-effector at the contact position.

Taking inner product of (10)~(12) with \dot{q} , \dot{x}_{obj} , and ω_{obj} , respectively, and summing them up, a Lyapunov-like energy function is obtained as follows:

$$\frac{d}{dt}E = \frac{d}{dt}(K + V_{end} + V_{com} + V_{gsp}) = -D \leq 0 \quad (13)$$

where

$$K = \frac{1}{2}\dot{q}^T H(q)\dot{q} + \frac{1}{2}\dot{x}_{obj}^T m_{obj}\dot{x}_{obj} + \frac{1}{2}\omega_{obj}^T I_{obj}\omega_{obj}, \quad (14)$$

$$V_{end} = \frac{1}{2} \sum_{i=1,2} k_{end} \Delta x_{end,i}^T \Delta x_{end,i}, \quad (15)$$

$$V_{com} = \frac{1}{2} k_{end} \Delta x_{com,i}^{(r)T} \Delta x_{com,i}^{(r)}, \quad (16)$$

$$V_{gsp} = \frac{1}{2} k_{gsp} \|x_{end,1} - x_{end,2}\|^2, \quad (17)$$

$$D = \dot{q}^T C \dot{q} + \sum_{i=1,2} c_{end} \dot{x}_{end,i}^T \dot{x}_{end,i} + c_{com} \dot{x}_{com,i}^{(r)T} \dot{x}_{com,i}^{(r)}. \quad (18)$$

K and D are the kinetic energy and the dissipated energy, respectively, and V_{end} , V_{com} and V_{gsp} are artificial potentials for end-effector regulation, CoM regulation and grasping control, respectively.

For a total artificial potential, $V = V_{end} + V_{com} + V_{gsp}$, there exists the non-negative minimum, $V_{min} \geq 0$, and thus, $E_{min} = K + V - V_{min} \geq 0$. Therefore, the following is satisfied:

$$\int_0^\infty D(t)dt = E(0) - E(\infty) \leq E(0) - E_{min} = (finite). \quad (19)$$

This means that $\dot{q}(t)$, $\dot{x}_{obj}(t)$, $\omega_{obj}(t) \in L^2(0, \infty)$, and finally leads the passivity of the whole system such that $\dot{q}(t)$, $\dot{x}_{obj}(t)$, $\omega_{obj}(t) \rightarrow 0$ as $t \rightarrow \infty$. Moreover, carefully chosen control gains can make the closed-loop system critically damped [22]. Thus, if the desired robot CoM from BP-Planner satisfies $x_{com,d}^{(r)} \in X_{com}^{(r)}$, it can be said that the total system never goes out of BoS while performing the given pick-and-place task.

IV. DYNAMIC SIMULATION RESULTS

A. Simulation Model of a Dual-arm Robot

In order to validate the proposed BP-CoM planner and whole-body controller, dynamic simulation is conducted. A commercial simulator, *Robotics Lab* from *SimLab Co.*, is

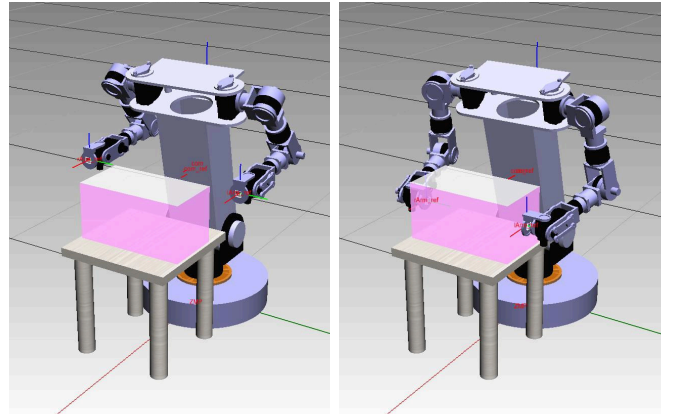


Fig. 7. Dynamic simulation model of a dual-arm robot for pick-and-place tasks

TABLE I

SEQUENTIAL END-EFFECTOR SET-POINTS FOR PICK-AND-PLACE TASKS

Time [s]	Normal task [m]	Extreme task [m]	Grasping
0.0	(0.3, 0.0, 0.6)	(0.3, 0.0, 0.6)	×
2.5	(0.4, 0.0, 0.5)	(0.8, 0.0, 0.8)	×
6.5	(0.4, 0.0, 0.5)	(0.8, 0.0, 0.8)	○
10.5	(0.3, 0.0, 0.6)	(0.3, 0.0, 0.6)	○
14.5	(0.4, 0.0, 0.5)	(0.8, 0.0, 0.8)	○
18.5	(0.4, 0.0, 0.5)	(0.8, 0.0, 0.8)	×

used in the simulation [24]. The dual-arm robot model has 2-DOF in torso and 8-DOF in each arm, and is in 36.72 kg weight and on a base plate with radius of 0.2 m (Fig. 7). A BP-CoM planner is designed as in Fig. 6 for this robot.

B. Simulation Results

Two different tasks to pick and place an object of 1 kg are assigned to the robot as shown in Table I; one is a normal case and the other is an extreme case. When the robot does not hold the object, $x_{com,d}^{(r)}$ is the same as $x_{com,d}^{(t)}$, but if the robot is grasping the object, $x_{com,d}^{(r)}$ is shifted back to the origin so that the total CoM could remain at the same position, thus not exceeding the border of the supporting polygon.

The simulation results show decent performance in both of manipulation task and whole-body balancing. Note that without the CoM binding effect, the desired total CoM would be assigned as 0.2 m in x-axis according to the proportional relation in Fig. 6, probably inducing a balance failure. However, by applying the BP-CoM planner, the robot maintains its balance even in the extreme case in spite of a bit inappropriate control gains with overshoot.

Fig. 9 shows the trajectories of the end-effector and the total CoM. The trajectories are quite similar to those of human motions, which demonstrates that the proposed controller in a simple form with low computational load still provides competitive, human-like motions.

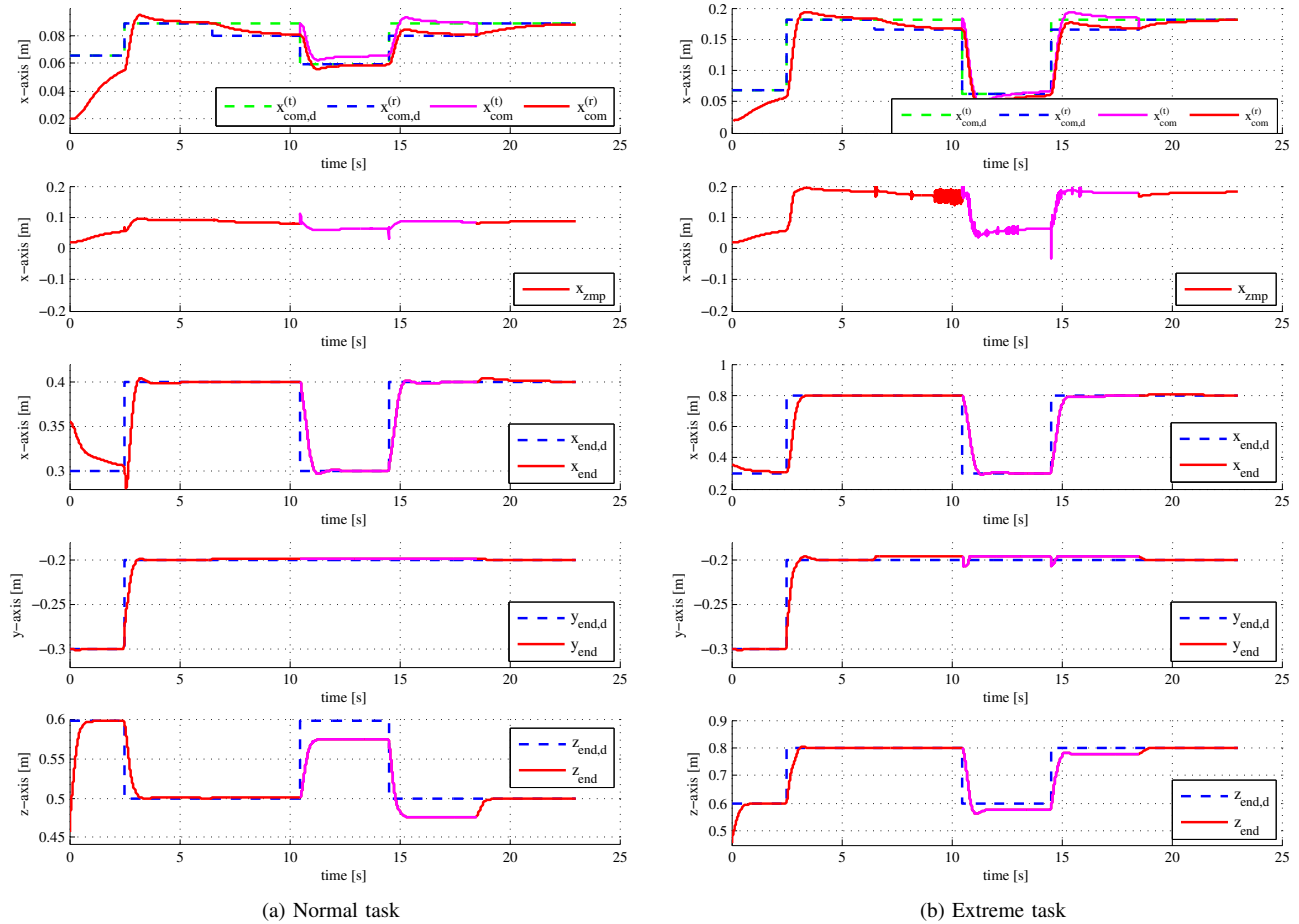


Fig. 8. Dynamic simulation results according to time for two different tasks. Magenta (light red) lines are when the robot grasps the object.

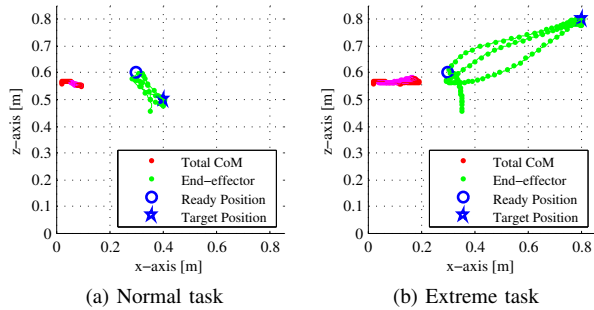


Fig. 9. Trajectories of the end-effector and the total CoM in the sagittal plane for two different tasks. Magenta (light red) lines are when the robot grasps the object.

V. CONCLUSION

This paper tackles an open problem on how to control the manipulation task and the whole-body balance simultaneously. Based on the human motion acquisition and analysis, human’s balance strategy during pick-and-place tasks is deduced, and this principle is implemented to a dual-arm robot control.

The bound-proportional CoM planner proposed in this paper shows a versatile capability that gives congenial CoM

commands to end-effector motions in a balance-safe region, while it gives conservative CoM commands despite demanding end-effector motions in a balance-marginal region.

In addition, dual-arm robot controller for whole-body balance and pick-and-place task is proposed based on task-space feedback and end-effector impedance control. While not many attempts have been made for such branched systems using this approach, the proposed controller demonstrated satisfactory results both in balance control and grasping control.

Still, there are many works to do in the future. This paper only dealt with planar motions in the sagittal plane. While the controller is generalized for 3-dimensional tasks, but the CoM planner has to be revised considering the effect of y and z-position of the target object. For this purpose, more exhaustive investigation on human motions for 3D pick-and-place tasks should be followed.

In the controller, for z-position regulation of the end-effector was not successful after grasping the object, additional compensation torque for object weight has to be applied. Moreover, the object mass is assumed to be given, but mass estimation function can be augmented using force-torque sensors at wrists.

REFERENCES

- [1] Y. Yamamoto and X. Yun, "Coordinating locomotion and manipulation of a mobile manipulator", *IEEE Transactions on Automatic Control*, vol. 39, no. 6, pp. 1326–1332, 1994.
- [2] C.P. Tang, P.T. Miller, V.N. Krovi, J. Ryu, S.K. Agrawal, et al., "Differential-flatness-based planning and control of a wheeled mobile manipulator—theory and experiment", *IEEE/ASME Transactions on Mechatronics*, no. 99, pp. 1–6, 2011.
- [3] T. Malheiro, T.D.N. Machado, S. Monteiro, W. Erlhagen, and E. Bicho, "Object transportation by a human and a mobile manipulator: a dynamical systems approach", in *Proceedings of 12th International Conference on Autonomous Robot Systems and Competitions (Robotica)*. 2012, pp. 27–32, Universidade do Minho.
- [4] D. Berenson, J. Kuffner, and H. Choset, "An optimization approach to planning for mobile manipulation", in *Proceedings of 2008 IEEE International Conference on Robotics and Automation (ICRA)*. Ieee, 2008, pp. 1187–1192.
- [5] N. Vahrenkamp, D. Berenson, T. Asfour, J. Kuffner, and R. Dillmann, "Humanoid motion planning for dual-arm manipulation and re-grasping tasks", in *Proceedings of 2009 IEEE/RSJ International Conference on Intelligent Robots and Systems (IROS)*. IEEE, 2009, pp. 2464–2470.
- [6] K. Harada, T. Foissotte, T. Tsuji, K. Nagata, N. Yamanobe, A. Nakamura, and Y. Kawai, "Pick and place planning for dual-arm manipulators", in *Proceedings of 2012 IEEE International Conference on Robotics and Automation (ICRA)*. IEEE, 2012, pp. 2281–2286.
- [7] Ikuo Mizuuchi, Masayuki Inaba, and Hirochika Inoue, "Adaptive pick-and-place behaviors in a whole-body humanoid robot with an autonomous layer based on parallel sensor-motor modules", *Robotics and Autonomous Systems*, vol. 28, no. 2–3, pp. 99 – 113, 1999.
- [8] S. Kajita, K. Yokoi, M. Saigo, and K. Tanie, "Balancing a humanoid robot using backdrive concerned torque control and direct angular momentum feedback", in *Proceedings of 2001 IEEE International Conference on Robotics and Automation (ICRA)*. IEEE, 2001, vol. 4, pp. 3376–3382.
- [9] K. Harada, S. Kajita, H. Saito, M. Morisawa, F. Kanehiro, K. Fujiwara, K. Kaneko, and H. Hirukawa, "A humanoid robot carrying a heavy object", in *Proceedings of 2005 IEEE International Conference on Robotics and Automation (ICRA)*. IEEE, 2005, pp. 1712–1717.
- [10] E. Yoshida, P. Blazevic, V. Hugel, K. Yokoi, and K. Harada, "Pivoting a large object: whole-body manipulation by a humanoid robot", *Applied Bionics and Biomechanics*, vol. 3, no. 3, pp. 227–235, 2006.
- [11] TR Kaminski, C. Bock, and AM Gentile, "The coordination between trunk and arm motion during pointing movements", *Experimental Brain Research*, vol. 106, no. 3, pp. 457–466, 1995.
- [12] C. Dean, R. Shepherd, and R. Adams, "Sitting balance i: trunk-arm coordination and the contribution of the lower limbs during self-paced reaching in sitting", *Gait & posture*, vol. 10, no. 2, pp. 135–146, 1999.
- [13] E. Rossi, A. Mitnitski, and A.G. Feldman, "Sequential control signals determine arm and trunk contributions to hand transport during reaching in humans", *The journal of physiology*, vol. 538, no. 2, pp. 659–671, 2002.
- [14] L.M. Nashner, "Practical biomechanics and physiology of balance", *Handbook of balance function and testing*, pp. 261–279, 1993.
- [15] T.D.J. Welch and L.H. Ting, "A feedback model reproduces muscle activity during human postural responses to support-surface translations", *Journal of neurophysiology*, vol. 99, no. 2, pp. 1032–1038, 2008.
- [16] S.K. Kim, J.H. Bae, Y. Oh, and S.R. Oh, "Concurrent control of position/orientation of a redundant manipulator based on virtual spring-damper hypothesis", in *Proceedings of 2011 IEEE International Conference on Robotics and Automation (ICRA)*. IEEE, 2011, pp. 6045–6050.
- [17] T. Bhattacharjee, Y. Oh, J.H. Bae, and S.R. Oh, "Controlling redundant robot arm-trunk systems for human-like reaching motion", in *Proceedings of 2010 IEEE/RSJ International Conference on Intelligent Robots and Systems (IROS)*. IEEE, 2010, pp. 2000–2005.
- [18] S.K. Kim, Y. Oh, and S.R. Oh, "Object manipulation in 3d space by two cone-shaped finger robots based on finger-thumb opposability without object sensing", in *Proceedings of 2012 IEEE International Conference on Robotics and Automation (ICRA)*. IEEE, 2012, pp. 5136–5141.
- [19] H.G. Armstrong, "Anthropometry and mass distribution for human analogues", *Military male aviators*, vol. 1, 1988.
- [20] Jong Hyeon Park, "Impedance control for biped robot locomotion", *IEEE Transactions on Robotics and Automation*, vol. 17, no. 6, pp. 870–882, 2001.
- [21] L. Sciavicco and B. Siciliano, "A solution algorithm to the inverse kinematic problem for redundant manipulators", *IEEE Journal of Robotics and Automation*, vol. 4, no. 4, pp. 403–410, 1988.
- [22] S. Arimoto and M. Sekimoto, "Human-like movements of robotic arms with redundant DOFs: virtual spring-damper hypothesis to tackle the Bernstein problem", in *Proceedings of 2006 IEEE International Conference on Robotics and Automation (ICRA)*, 2006, pp. 1860 – 1866.
- [23] S. Arimoto, K. Tahara, JH Bae, and M. Yoshida, "A stability theory of a manifold: concurrent realization of grasp and orientation control of an object by a pair of robot fingers", *Robotica*, vol. 21, no. 2, pp. 163–178, 2003.
- [24] RoboticsLab: Robotics S/W Development Environment including Dynamics and Control Engines. (<http://www.rlab.co.kr>).